# Multidimensional Index Modulation in Wireless Communications

Bharath Shamasundar, Swaroop Jacob, Sandeep Bhat, and A. Chockalingam
Department of Electrical Communication Engineering
Indian Institute of Science, Bangalore 560012, India

***Abstract*—In index modulation schemes, information bits are conveyed through indexing of transmission entities such as antennas, subcarriers, times slots, precoders, subarrays, and radio frequency (RF) mirrors. Index modulation schemes are attractive for their advantages such as good performance, high rates, and hardware simplicity. This paper focuses on index modulation schemes in which multiple transmission entities, namely, *antennas*, *time slots*, and *RF mirrors*, are indexed *simultaneously*. Recognizing that such multidimensional index modulation schemes encourage sparsity in their transmit signal vectors, we propose efficient signal detection schemes that use compressive sensing based reconstruction algorithms. Results show that, for a given rate, improved performance is achieved when the number of indexed transmission entities is increased. We also explore indexing opportunities in *load modulation*, which is a modulation scheme that offers power efficiency and reduced RF hardware complexity advantages in multiantenna systems. Results show that indexing space and time in load modulated multiantenna systems can achieve improved performance.**

***keywords:*** *Multidimensional index modulation, transmit antennas, transmit RF chains, time slots, RF mirrors, indexed load modulation, multidimensional hypersphere, signal detection, compressive sensing.*

## I. Introduction

Conventional modulation schemes convey information bits by sending symbols from complex modulation alphabets such as quadrature amplitude modulation (QAM) and phase shift keying (PSK) signal sets. In addition to the bits conveyed by complex modulation symbols, the indices of transmission entities such as transmit antennas, time slots, subcarriers, subarrays, etc., which get activated during data transmission can convey additional information bits. Modulation schemes in which bits are conveyed through such indexing are referred to as index modulation schemes [1]. Several index modulation schemes and their performance are being reported extensively in the recent literature.

A popular index modulation scheme in the literature is spatial modulation, where transmit antennas are indexed to convey information bits [2]-[4]. In its basic form, spatial modulation (SM) activates only one among the available transmit antennas at a time, and which antenna gets activated conveys information bit(s). Since only one transmit RF chain is adequate for its operation, SM has the RF hardware simplicity advantage. A generalized version of SM, referred to as generalized spatial modulation (GSM) [5]-[7], allows simultaneous activation of more than one antenna at a time, and which antennas are activated convey information bits. GSM has the advantage of achieving higher rates and better performance than SM and spatial multiplexing [6]. SM and GSM employed in a multiuser MIMO setting on the uplink have been shown to offer attractive performance compared to conventional modulation [8]-[11]. Similar to indexing antennas, subarrays in an antenna array can be indexed. Such an indexing scheme, termed as subarray index modulation, can be attractive in mmWave communication [12],[13].

Subcarrier index modulation schemes index subcarriers in multicarrier systems [14]-[20]. For example, in an OFDM based subcarrier index modulation scheme, not all subcarriers in an OFDM frame carry modulation symbols, and which subcarriers among the available subcarriers carry symbols convey additional information bits. Equivalently, in the time domain, time slots in a frame can be indexed in block transmission systems [21]. That is, some time slots in a frame can be left unused by design so that the indices of the used-time slots convey information bits. In precoder index modulation [22],[23], the transmitter is provided with a set of pseudo-random precoder matrices, and, at a time, one among them is chosen and used. The index of the precoder used conveys information bits.

The use of parasitic elements for signaling is getting popular because of its advantages that include improved performance [24],[25]. Media-based modulation (MBM) is one such scheme [26]-[29]. MBM uses digitally controlled (ON/OFF) parasitic elements external to the transmit antenna that act as RF mirrors to create different channel fade realizations which are used as the channel modulation alphabet, and uses indexing of these RF mirrors to convey information bits. An advantage of MBM is that the number of bits conveyed through indexing of RF mirrors grows linearly with the number of mirrors used. This is in contrast with SM schemes where the number of index bits grow only logarithmically in number of antennas. MBM signal vectors have good distance properties, and this enables MBM to achieve better performance compared to conventional modulation schemes.

Motivated by the performance gains that can be potentially realized through the use of index bits, in this paper, we investigate index modulation schemes in which multiple transmission entities, namely, antennas, time slots, and RF mirrors, are indexed simultaneously. Specifically, we consider 1) time-indexed spatial modulation (TI-SM), where time slots

This work was supported in part by the J. C. Bose National Fellowship, Department of Science and Technology, Government of India.

and transmit antennas are indexed, 2) time-indexed media-based modulation (TI-MBM), where time slots and RF mirrors are indexed, 3) spatial modulation–media-based modulation (SM-MBM), where transmit antennas and RF mirrors are indexed, and 4) time-indexed SM-MBM (TI-SM-MBM), where time slots, transmit antennas, and RF mirrors are indexed simultaneously. We also propose efficient signal detection schemes that use compressive sensing based reconstruction algorithms that exploit the sparsity that is inherently present in the signal vectors of these schemes. It is found that, for a given rate, improved performance can be achieved when more transmission entities are indexed.

Recently, the concept of *load modulation arrays* is getting recognized as a promising approach to realizing massive antenna arrays with low RF front-end hardware complexity [30],[31]. It eliminates the need for traditional RF upconversion modules (superheterodyne or zero-IF) consisting of DACs, mixers, and filters, and requires only one transmit power amplifier (PA) for any number of transmit antennas. It achieves this by directly varying ('modulating') the antenna impedances (load impedances) that control the antenna currents. While the RF complexity advantages of this modulation scheme have been articulated well recently, its performance aspects need more investigations. In this light, we investigate the potential role that indexing can play in improving performance. Our results are positive in this regard. In particular, we investigate *indexed load modulation* schemes, where we index space and time. Our performance results show that spatial indexing and time indexing in load modulated multiantenna systems can achieve improved performance.

The rest of the paper is organized as follows. Multidimensional modulation schemes that index antennas, time slots, and RF mirrors are presented in Sec. II. Compressive sensing based algorithms for detection of multidimensional index modulation signals are presented in Sec. III. Indexed load modulation schemes are presented in Sec. IV. Conclusions are presented in Sec. V.

## II. Multidimensional index modulation schemes

In this section, we consider multidimensional index modulation schemes in which combinations of antennas, time slots, and RF mirrors are indexed simultaneously. The considered schemes include 1) TI-SM scheme, where time slots and transmit antennas are indexed, 2) TI-MBM scheme, where time slots and RF mirrors are indexed, 3) SM-MBM scheme, where transmit antennas and RF mirrors are indexed, and 4) TI-SM-MBM scheme, where time slots, transmit antennas, and RF mirrors are indexed simultaneously. Figure 1 shows the generalized block diagram of the multidimensional index modulation scheme. The notations for various system parameters used throughout the paper are listed in Table I.

### A. Time-indexed spatial modulation (TI-SM)

In TI-SM, indexing is done across time and space (i.e., across time slots and antennas) [33]. The TI-SM scheme has $n_t$ transmit antennas and one transmit RF chain. Figure 1 specializes to TI-SM if RF mirrors and the RF mirror control switch are removed. Information bits are conveyed through time-slot indexing, antenna indexing, and QAM/PSK symbols. The channel between a transmit-receive antenna pair is assumed to be frequency-selective with $L$ multipaths. Time-slot and antenna indexing are done as follows.

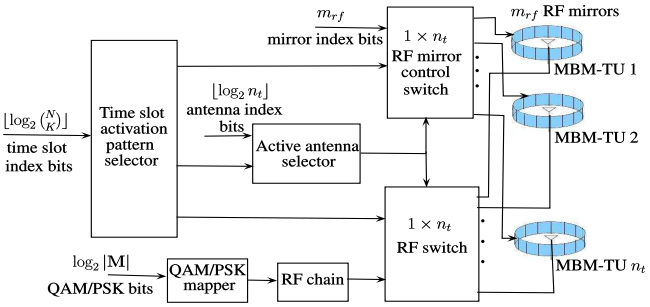


Fig. 1. Multidimensional index modulation scheme.

| | |
|---|---|
| $n_t$ | Number of transmit antennas |
| $n_r$ | Number of receive antennas |
| $m_{rf}$ | Number of RF mirrors per transmit antenna |
| $M \triangleq 2^{m_{rf}}$ | Number of possible mirror activation patterns (MAP) |
| $n_L$ | Number of load modulation transmit units (LM-TU) |
| $n_K$ | Number of active LM-TUs |
| $n_M$ | Number of vectors in the load modulation alphabet |
| $N$ | Length of the data part of a frame in no. of time slots |
| $K$ | Number of active time slots per frame |
| $L$ | Number of multipaths |
| $\mathbb{M}$ | Conventional modulation alphabet |
| $\mathbb{T}$ | Set of all valid time-slot activation patterns (TAP) |
| $\mathbb{L}$ | Set of all valid LM-TU activation patterns (LAP) |
| $\mathbf{t}^{\mathbf{x}}$ | TAP corresponding to signal vector $\mathbf{x}$ |
| $\mathbf{q}^{\mathbf{x}}$ | LAP corresponding to signal vector $\mathbf{x}$ |
| $\mathbb{S}_{\text{sm}}$ | Spatial modulation (SM) signal set |
| $\mathbb{S}_{\text{mbm}}$ | Media-based modulation (MBM) signal set |
| $\mathbb{S}_{\text{ti-sm}}$ | Time-indexed SM (TI-SM) signal set |
| $\mathbb{S}_{\text{ti-mbm}}$ | Time-indexed MBM (TI-MBM) signal set |
| $\mathbb{S}_{\text{sm-mbm}}$ | SM-MBM signal set |
| $\mathbb{S}_{\text{ti-sm-mbm}}$ | TI-SM-MBM signal set |
| $\mathbb{S}_{\text{lm}}$ | Load modulation (LM) alphabet |
| $\mathbb{S}_{\text{si-lm}}$ | Spatially-indexed LM (SI-LM) alphabet |
| $\mathbb{S}_{\text{ti-lm}}$ | Time-indexed LM (TI-LM) alphabet |
| $\eta$ | Achieved rate in bits per channel use (bpcu) |

TABLE I

*1) Time-slot indexing:* Time is divided into frames. Each frame consists of $N+L-1$ time-slots, where $N$ is the length of the data part of the frame in number of time slots, and $L-1$ is the number of time slots used for transmitting cyclic prefix (CP). Out of $N$ time slots, only $K$ time slots, $1 \leq K \leq N$, are used for data transmission. The choice of which $K$ slots among the $N$ slots are selected for transmission conveys $\lfloor \log_2 \binom{N}{K} \rfloor$ information bits. These bits are called 'time index bits' and the selected time slots are called 'active slots' in the frame. An $N$-length pattern of active/inactive status of the slots in a frame is called a 'time-slot activation pattern' (TAP). There are $\binom{N}{K}$ possible TAPs, of which $2^{\lfloor \log_2 \binom{N}{K} \rfloor}$ are used and they form the set of valid TAPs.

*Example:* Consider $N = 4, K = 2$. We have $\binom{N}{K} = 6$, $2^{\lfloor \log_2 \binom{N}{K} \rfloor} = 4$. Out of the six possible TAPs, the following four TAPs can be taken as the valid TAPs for signaling –

$\{[1\ 0\ 0\ 1], [1\ 0\ 1\ 0], [0\ 1\ 0\ 1], [1\ 1\ 0\ 0]\}$, where '1' indicates an active slot and '0' indicates an inactive slot.

*2) Antenna indexing:* In each active slot, one transmit antenna out of $n_t$ antennas is selected based on $\lfloor \log_2 n_t \rfloor$ bits. These bits are called 'antenna index bits' and the antenna selected is called the 'active antenna' in that slot. Note that in a TI-SM frame, the active antenna can be different in each of the active slots. Also, none of the antennas are active in an inactive slot. Since $K$ out of $N$ time slots are active in a frame, $K\lfloor \log_2 n_t \rfloor$ information bits are conveyed through antenna indexing in one frame. Further, a symbol from a conventional modulation alphabet $\mathbb{M}$ (say, QAM or PSK) is transmitted from the active antenna in an active slot. This conveys $\log_2 |\mathbb{M}|$ bits in each active time slot. Hence, $K \log_2 |\mathbb{M}|$ bits are conveyed in a frame by conventional modulation symbols. Thus, in each active time slot in a frame, an $n_t \times 1$ SM signal vector is transmitted. The achieved rate in TI-SM scheme is therefore given by

$$\eta_{\text{ti-sm}} = \frac{1}{N+L-1}\left\{ \left\lfloor \log_2 \binom{N}{K} \right\rfloor + K\big( \lfloor \log_2 n_t \rfloor + \log_2 |\mathbb{M}| \big) \right\} \text{ bpcu.} \quad (1)$$

*3) TI-SM signal set:* As noted earlier, an $n_t \times 1$ SM signal vector is transmitted in an active time slot of a frame, and nothing gets transmitted in an inactive slot. The SM signal set is given by

$$\mathbb{S}_{\text{sm}} = \{\mathbf{s}_{j,l} : j = 1, \cdots, n_t,\ l = 1, \cdots, |\mathbb{M}|\}$$
$$\text{s.t } \mathbf{s}_{j,l} = [0 \cdots 0 \underbrace{s_l}_{j\text{th coordinate}} 0 \cdots 0]^T,\ \ s_l \in \mathbb{M}. \quad (2)$$

For example, if $n_t = 4$ and $|\mathbb{M}| = 2$ (i.e., BPSK), then the SM signal set is given by

$$\mathbb{S}_{\text{sm}} = \left\{ \begin{bmatrix}1\\0\\0\\0\end{bmatrix}, \begin{bmatrix}-1\\0\\0\\0\end{bmatrix}, \begin{bmatrix}0\\1\\0\\0\end{bmatrix}, \begin{bmatrix}0\\-1\\0\\0\end{bmatrix}, \begin{bmatrix}0\\0\\1\\0\end{bmatrix}, \begin{bmatrix}0\\0\\-1\\0\end{bmatrix}, \begin{bmatrix}0\\0\\0\\1\end{bmatrix}, \begin{bmatrix}0\\0\\0\\-1\end{bmatrix} \right\}. \quad (3)$$

Let $\mathbf{x}_1, \mathbf{x}_2, \cdots, \mathbf{x}_N$ denote the transmitted signal vectors in $N$ slots. The TI-SM signal set then can be written as

$$\mathbb{S}_{\text{ti-sm}} = \{\mathbf{x} = [\mathbf{x}_1^T \mathbf{x}_2^T \cdots \mathbf{x}_N^T]^T : \mathbf{x}_i \in \mathbb{S}_{\text{sm}} \cup \mathbf{0}, \|\mathbf{x}\|_0 = K \text{ and } \mathbf{t}^{\mathbf{x}} \in \mathbb{T}\}, \quad (4)$$

where $\mathbf{0}$ denotes $n_t \times 1$ zero vector, $\mathbb{T}$ denotes the set of all valid TAPs, and $\mathbf{t}^{\mathbf{x}}$ denotes the TAP corresponding to the signal vector $\mathbf{x}$. The size of TI-SM signal set is $|\mathbb{S}_{\text{ti-sm}}| = 2^{\lfloor \log_2 \binom{N}{K} \rfloor} (n_t |\mathbb{M}|)^K$. For example, if $N = 4, K = 2, n_t = 4, |\mathbb{M}| = 4$, then $|\mathbb{S}_{\text{ti-sm}}| = 1024$. An $Nn_t \times 1$ TI-SM signal vector from $\mathbb{S}_{\text{ti-sm}}$ is transmitted over $N$ slots in a frame.

*4) TI-SM received signal:* We assume that the channel remains invariant for one frame duration. Let $n_r$ denote the number of receive antennas at the receiver. Assuming perfect channel knowledge at the receiver, after removing the CP, the $Nn_r \times 1$ received signal vector can be written as

$$\mathbf{y} = \mathbf{H}\mathbf{x} + \mathbf{n}, \quad (5)$$

where $\mathbf{n}$ is $Nn_r \times 1$ noise vector with $\mathbf{n} \sim \mathcal{CN}(\mathbf{0}, \sigma^2 \mathbf{I})$ and $\mathbf{H}$ is $Nn_r \times Nn_t$ equivalent block circulant matrix given by

$$\mathbf{H} = \begin{bmatrix} \mathbf{H}_0 & \mathbf{0} & \mathbf{0} & \cdots & \mathbf{H}_{L-1} & \cdots & \mathbf{H}_1 \\ \mathbf{H}_1 & \mathbf{H}_0 & \mathbf{0} & \cdots & \mathbf{0} & \cdots & \mathbf{H}_2 \\ \vdots & & & \vdots & & & \\ \mathbf{H}_{L-1} & \mathbf{H}_{L-2} & \cdots & \mathbf{H}_0 & \mathbf{0} & \cdots & \mathbf{0} \\ \mathbf{0} & \mathbf{H}_{L-1} & \cdots & \mathbf{H}_1 & \mathbf{H}_0 & \cdots & \mathbf{0} \\ \vdots & & & \vdots & & & \\ \mathbf{0} & \mathbf{0} & \cdots & \cdots & \cdots & \cdots & \mathbf{H}_0 \end{bmatrix}, \quad (6)$$

where $\mathbf{H}_l$ denotes the $n_r \times n_t$ channel matrix corresponding to the $l$th multipath, $l = 0, \cdots, L-1$. Uniform power delay profile is assumed such that $\mathbf{h}_l^k \sim \mathcal{CN}(\mathbf{0}, \frac{1}{L}\mathbf{I})$, where $\mathbf{h}_l^k$ is the $k$th column of $\mathbf{H}_l$.

### *B. Time-indexed media-based modulation (TI-MBM)*

In this section, we consider TI-MBM. In TI-MBM, indexing is done across time slots and RF mirrors [34]. The TI-MBM transmitter consists of one transmit antenna (i.e., $n_t = 1$) and $m_{rf}$ RF mirrors placed near it. The transmit antenna and its $m_{rf}$ RF mirrors are together called an 'MBM transmit unit' (MBM-TU). Figure 1 specializes to TI-MBM by using only one MBM-TU and removing the RF switch. Bits are conveyed through time-slot indexing, RF mirror indexing, and QAM/PSK symbols. Time-slot indexing is done in the same way as in TI-SM. A symbol from the alphabet $\mathbb{M}$ gets sent in each active time slot.

*1) RF mirror indexing:* The propagation environment near the transmit antenna in each active slot is controlled by the ON/OFF status of the $m_{rf}$ RF mirrors. The ON/OFF status of the $m_{rf}$ mirrors is controlled by $m_{rf}$ information bits. These bits are called the 'mirror index bits'. An $m_{rf}$-length pattern of ON/OFF status of the mirrors in an active slot is called a 'mirror activation pattern' (MAP). In an active slot, one of the $2^{m_{rf}}$ MAPs is selected using $m_{rf}$ information bits. A mapping is done between the combinations of $m_{rf}$ information bits and the MAPs. The mapping between the MAPs and information bits is made known a priori to both the transmitter and the receiver for encoding and decoding purposes, respectively. In each active time slot in a frame, a $2^{m_{rf}} \times 1$ MBM signal vector is transmitted. The achieved rate in TI-MBM scheme is therefore given by

$$\eta_{\text{ti-mbm}} = \frac{1}{N+L-1}\left\{ \left\lfloor \log_2 \binom{N}{K} \right\rfloor + K\big( m_{rf} + \log_2 |\mathbb{M}| \big) \right\} \text{ bpcu.} \quad (7)$$

It is noted that the conventional MBM without time-slot indexing becomes a special case of TI-MBM when $K = N$.

*2) TI-MBM signal set:* Define $\mathbb{M}_0 \triangleq \mathbb{M} \cup 0$ and $M \triangleq 2^{m_{rf}}$. The conventional MBM signal set, denoted by $\mathbb{S}_{\text{mbm}}$, is the set of $M \times 1$-sized MBM signal vectors, which is given by

$$\mathbb{S}_{\text{mbm}} = \left\{ \mathbf{s}_{k,q} \in \mathbb{M}_0^M : k = 1, \cdots, M,\ q = 1, \cdots, |\mathbb{M}| \right\}$$
$$\text{s.t } \mathbf{s}_{k,q} = [0 \cdots 0 \underbrace{s_q}_{k\text{th coordinate}} 0 \cdots 0]^T,\ s_q \in \mathbb{M}, \quad (8)$$

where $k$ is the index of the MAP. The size of the MBM signal set is $|\mathbb{S}_{\text{mbm}}| = M|\mathbb{M}|$. For example, for $m_{rf} = 2$ and $|\mathbb{M}| = 2$ (i.e., BPSK), the MBM signal set is given by

$$\mathbb{S}_{\text{mbm}} = \left\{ \begin{bmatrix}1\\0\\0\\0\end{bmatrix}, \begin{bmatrix}-1\\0\\0\\0\end{bmatrix}, \begin{bmatrix}0\\1\\0\\0\end{bmatrix}, \begin{bmatrix}0\\-1\\0\\0\end{bmatrix}, \begin{bmatrix}0\\0\\1\\0\end{bmatrix}, \begin{bmatrix}0\\0\\-1\\0\end{bmatrix}, \begin{bmatrix}0\\0\\0\\1\end{bmatrix}, \begin{bmatrix}0\\0\\0\\-1\end{bmatrix} \right\}. \quad (9)$$

Let $\mathbf{x}_1, \mathbf{x}_2, \cdots, \mathbf{x}_N$ denote the transmitted signal vectors in $N$ slots. The TI-MBM signal set then can be written as

$$\begin{aligned}\mathbb{S}_{\text{ti-mbm}} \;=\; \{\mathbf{x} = [\mathbf{x}_1^T \mathbf{x}_2^T \cdots \mathbf{x}_N^T]^T : \mathbf{x}_j \in \mathbb{S}_{\text{mbm}} \cup \mathbf{0},\\ \|\mathbf{x}\|_0 = K \text{ and } \mathbf{t}^{\mathbf{x}} \in \mathbb{T}\}, \end{aligned} \quad (10)$$

where $\mathbb{T}$ denotes the set of valid TAPs and $\mathbf{t}^{\mathbf{x}}$ denotes the TAP corresponding to $\mathbf{x}$. The size of the TI-MBM signal set is $|\mathbb{S}_{\text{ti-mbm}}| = 2^{\lfloor \log_2 \binom{N}{K} \rfloor} (M|\mathbb{M}|)^K$. An $NM \times 1$ TI-MBM signal vector from $\mathbb{S}_{\text{ti-mbm}}$ is transmitted over $N$ slots in a frame.

*3) TI-MBM received signal:* Let $h^j(l,k)$ denote the channel gain from the transmit MBM-TU to the $j$th receive antenna on the $l$th multipath for the $k$th MAP, where $h^j(l,k) \sim \mathcal{CN}(0, \frac{1}{L})$. Assume that the channel remains invariant over one frame duration and assume perfect timing and channel knowledge at the receiver. After removing the CP, the $Nn_r \times 1$-sized received signal vector $\mathbf{y}$ can be written as $\mathbf{y} = \mathbf{H}\mathbf{x} + \mathbf{n}$, where $\mathbf{n}$ is the noise vector of size $Nn_r \times 1$ with $\mathbf{n} \sim \mathcal{CN}(\mathbf{0}, \sigma^2\mathbf{I})$, and $\mathbf{H}$ is the $Nn_r \times NM$ equivalent block circulant matrix of the same form as (6), with $\mathbf{H}_l$ being the $n_r \times M$ channel matrix corresponding to the $l$th multipath.

### C. Spatial modulation–media-based modulation (SM-MBM)

In this section, we consider SM-MBM. In SM-MBM, indexing is done across MBM-TUs and RF mirrors. The SM-MBM transmitter has $n_t$ MBM-TUs and one RF chain. Figure 1 specializes to SM-MBM by removing the time-slot activation pattern selector, as indexing in time is not involved in SM-MBM. Bits are conveyed through MBM-TU indexing, RF mirror indexing, and QAM/PSK symbols.

In SM-MBM, all the $N$ time slots in a frame are used for transmission. In each time slot, one out of $n_t$ MBM-TUs is selected based on $\lfloor \log_2 n_t \rfloor$ bits, and an $n_t \times 1$ SM signal vector from $\mathbb{S}_{\text{sm}}$ gets transmitted across $n_t$ MBM-TUs. The $m_{rf}$ mirrors near the active MBM-TU are made ON/OFF depending on the MAP chosen based on $m_{rf}$ bits. Therefore, in addition to the bits conveyed by the SM vector, the different channel fade realizations created by the RF mirrors in the active MBM-TU also convey bits through the MAP index. Hence, the achieved rate in SM-MBM is given by

$$\eta_{\text{sm-mbm}} = \frac{N}{N+L-1}\left\{ \lfloor \log_2 n_t \rfloor + m_{rf} + \log_2 |\mathbb{M}| \right\}. \quad (11)$$

*1) SM-MBM signal set:* The SM-MBM signal set, denoted by $\mathbb{S}_{\text{sm-mbm}}$, is given by

$$\begin{aligned}\mathbb{S}_{\text{sm-mbm}} \;=\; \{\mathbf{z} = [\mathbf{z}_1^T \mathbf{z}_2^T \cdots \mathbf{z}_{n_t}^T]^T : \mathbf{z}_j = s_j \mathbf{e}_{l_j},\\ l_j \in \{1, \cdots, M\} \text{ and } \mathbf{s} = [s_1 s_2 \cdots s_{n_t}]^T \in \mathbb{S}_{\text{sm}}\}, \end{aligned} \quad (12)$$

where $s_j \in \mathbb{M} \cup 0$, $l_j$ is the index of the MAP chosen on the $j$th MBM-TU, and $\mathbf{e}_{l_j}$ is an $M \times 1$ vector whose $l_j$th coordinate is '1' and all other coordinates are zero. Note that the length of a SM-MBM signal vector is $n_t M \times 1$, and the size of SM-MBM signal set is $|\mathbb{S}_{\text{sm-mbm}}| = n_t M|\mathbb{M}|$. The transmit vector in $N$ time slots of a TI-SM frame is an $Nn_tM \times 1$ vector given by $\mathbf{x} = [\mathbf{x}_1^T \mathbf{x}_2^T \cdots \mathbf{x}_N^T]^T$, where $\mathbf{x}_i \in \mathbb{S}_{\text{sm-mbm}}$. The number of possible transmit vectors in a frame is $(n_t M|\mathbb{M}|)^N$.

*2) SM-MBM received signal:* Let $h^{(j,i)}(l,k)$ denote the channel gain from from the $i$th MBM-TU to the $j$th receive antenna on the $l$th multipath for the $k$th MAP, where $h^{(j,i)}(l,k) \sim \mathcal{CN}(0, \frac{1}{L})$. In each slot, an SM-MBM signal vector from $\mathbb{S}_{\text{sm-mbm}}$ is sent. At the receiver, after removing the CP, the $Nn_r \times 1$ received signal vector $\mathbf{y}$ can be written as $\mathbf{y} = \mathbf{H}\mathbf{x} + \mathbf{n}$, where $\mathbf{n}$ is the $Nn_r \times 1$ noise vector with $\mathbf{n} \sim \mathcal{CN}(0, \sigma^2\mathbf{I})$, and $\mathbf{H}$ is the $Nn_r \times Nn_tM$ equivalent block circulant channel matrix of the form (6), with $\mathbf{H}_l$ being the $n_r \times n_tM$ channel matrix corresponding to the $l$th multipath.

### D. Time-indexed SM-MBM (TI-SM-MBM)

In this section, we consider TI-SM-MBM, which is a generalized scheme of which TI-SM, TI-MBM, and SM-MBM are special cases. In TI-SM-MBM, time slots, antennas, and RF mirrors are indexed simultaneously (see Fig. 1). The TI-SM-MBM scheme has $n_t$ MBM-TUs and one transmit RF chain. Time indexing is done by choosing $K$ out of $N$ time slots in a frame as active slots, based on $\lfloor \log_2 \binom{N}{K} \rfloor$ bits. In an active time slot, one of the $n_t$ MBM-TUs is selected based on $\lfloor \log_2 n_t \rfloor$ bits and activated. The RF mirrors associated with the active MBM-TU are controlled by $m_{rf}$ bits that select a MAP. A symbol from $\mathbb{M}$ is transmitted from the active MBM-TU in an active time slot. Therefore, the achieved rate in TI-SM-MBM scheme is given by

$$\begin{aligned}\eta_{\text{ti-sm-mbm}} = \frac{1}{N+L-1}\Bigg\{ \left\lfloor \log_2 \binom{N}{K} \right\rfloor + K\big( \lfloor \log_2 n_t \rfloor\\ + m_{rf} + \log_2 |\mathbb{M}| \big) \Bigg\} \text{ bpcu}. \end{aligned} \quad (13)$$

*1) TI-SM-MBM signal set:* In TI-SM-MBM, an SM-MBM signal vector from $\mathbb{S}_{\text{sm-mbm}}$ in (12) is transmitted in an active time slot and nothing gets transmitted in an inactive time slot. Let $\mathbf{x}_1, \mathbf{x}_2, \cdots, \mathbf{x}_N$ denote the transmit vectors in $N$ slots. The TI-SM-MBM signal set is then given by

$$\begin{aligned}\mathbb{S}_{\text{ti-sm-mbm}} =& \{\mathbf{x} = [\mathbf{x}_1^T \mathbf{x}_2^T \cdots \mathbf{x}_N^T]^T : \mathbf{x}_j \in \mathbb{S}_{\text{sm-mbm}} \cup \mathbf{0},\\ &\|\mathbf{x}\|_0 = K \text{ and } \mathbf{t}^{\mathbf{x}} \in \mathbb{T}\}, \end{aligned} \quad (14)$$

where $\mathbf{0}$ denotes the $n_tM \times 1$ zero vector, $\mathbf{t}^{\mathbf{x}}$ is the TAP of $\mathbf{x}$ and $\mathbb{T}$ is the set of all valid TAPs. The length of a TI-SM-MBM signal vector is thus $Nn_tM \times 1$. Note that there are only $K$ non-zero elements out of $Nn_tM$ elements in a TI-SM-MBM signal vector, whose positions are decided by the chosen TAP, MAP, and active MBM-TU index. The size of the TI-SM-MBM signal set is $|\mathbb{S}_{\text{ti-sm-mbm}}| = 2^{\lfloor \log_2 \binom{N}{K} \rfloor}(n_tM|\mathbb{M}|)^K$. A signal vector from $\mathbb{S}_{\text{ti-sm-mbm}}$ is transmitted in a frame. It can be seen that TI-SM, TI-MBM, and SM-MBM become special

cases of TI-SM-MBM when $i)$ $K < N$, $n_t > 1$, $m_{rf} = 0$, $ii)$ $K < N$, $n_t = 1$, $m_{rf} \geq 1$, and $iii)$ $K = N$, $n_t > 1$, $m_{rf} \geq 1$, respectively.

*2) TI-SM-MBM received signal:* At the receiver, after removing the CP, the $Nn_r \times 1$ received signal vector $\mathbf{y}$ can be written as $\mathbf{y} = \mathbf{H}\mathbf{x} + \mathbf{n}$, where $\mathbf{x} \in \mathbb{S}_{\text{ti-sm-mbm}}$ is the transmit vector of size $Nn_tM \times 1$, and $\mathbf{n}$ and $\mathbf{H}$ are as defined for SM-MBM.

### *E. ML detection performance*

In Fig. 2, we present the BER performance of the TI-SM, TI-MBM, SM-MBM, and TI-SM-MBM schemes under ML detection for $N = 4$, $L = 2$, and $n_r = 8$. Note that in all the four schemes only one transmit RF chain is used. All the four schemes are configured such that they achieve the same rate of 3.2 bpcu. Also, for the time-indexed schemes (i.e., for TI-SM, TI-MBM, TI-SM-MBM) $K$ is taken to be 2. To achieve 3.2 bpcu rate, TI-SM scheme uses $n_t = 4$ and 32-QAM, TI-MBM uses $n_t = 1$, $m_{rf} = 3$, and 16-QAM, SM-MBM uses $n_t = 4$, $m_{rf} = 1$, and BPSK, and TI-SM-MBM uses $n_t = 4$, $m_{rf} = 3$, and 4-QAM. The following observations can be made from Fig. 2.

- First, a comparison between TI-SM and TI-MBM shows that MBM with time indexing can be more attractive compared to SM with time indexing (about 2 dB advantage at $10^{-3}$ BER). This is because to match the bpcu, SM needs more antennas and/or increased QAM-size which can lead to relatively poor performance as observed in the figure. Note that $n_t = 4$ and QAM-size is 32 for TI-SM, whereas $n_t = 1$ and QAM-size is 16 for TI-MBM. The linear increase in rate as a function of number of mirrors in MBM allows this QAM-size reduction.
- Next, SM-MBM is found to outperform both TI-SM and TI-MBM (about 5.8 dB and 3.8 dB advantage, respectively, at $10^{-3}$ BER). This can be attributed to the fact that time-indexed schemes incur a rate loss due to inactive time slots, and to compensate this loss the QAM-size and/or number of antennas and/or number of RF mirrors have to be increased in order to match the bpcu. This explains why TI-SM and TI-MBM need 32-QAM and 16-QAM, respectively, to achieve 3.2 bpcu. Whereas, SM-MBM achieves the same rate using just BPSK. On the other hand, time indexing offers the advantage of reduced inter-symbol interference (ISI) due to inactive slots. Here, the degrading effect of increased QAM-size dominates the beneficial effect of reduced ISI.
- Finally, TI-SM-MBM in which indexing is done on all the three entities (time slots, antennas, RF mirrors) is the most attractive (about 7.2 dB, 5.2 dB, and 1.4 dB advantage at $10^{-3}$ BER compared to TI-SM, TI-MBM, and SM-MBM, respectively). Note that using time indexing on top of SM-MBM turns out to be advantageous compared to SM-MBM without time indexing. This is because, here, the beneficial effect of reduced ISI due to time indexing is more compared to the degrading effect of QAM-size increase from BPSK to 4-QAM.

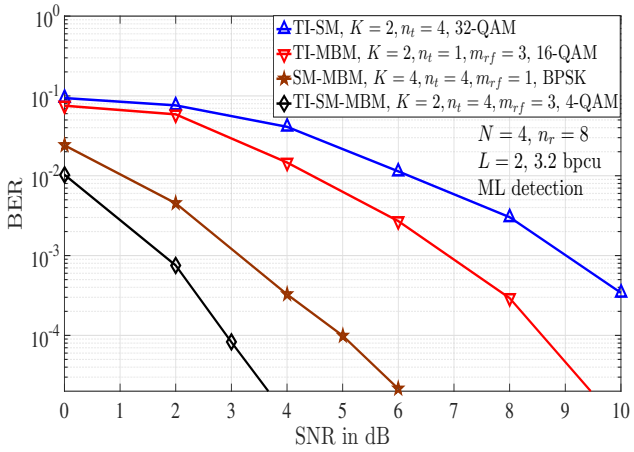


Fig. 2. BER performance of TI-SM, TI-MBM, SM-MBM, and TI-SM-MBM schemes with 3.2 bpcu under ML detection, $N = 4$, $L = 2$, $n_r = 8$.

The above observations and discussions illustrate that indexing multiple entities with a careful choice of system configuration/parameters exploiting the underlying tradeoffs involved can be beneficial. Further, note that ML detection becomes prohibitively complex for large-dimension signals because of the exponential complexity. We exploit the inherent sparsity in the indexed transmit vectors to devise low-complexity compressive sensing based detection algorithms.

## III. Compressive Sensing Based Detection

It is noted that the transmit vectors in the multidimensional index modulation schemes presented in the previous section are inherently sparse. This can be seen from their signal sets defined in (4), (10), (12), and (14). As a specific example, consider TI-SM-MBM with $N = 16, K = 6, n_t = 4$, and $m_{rf} = 4$. While the length of each transmit vector is $Nn_tM = 16 \times 4 \times 2^4 = 1024$, there are only $K = 6$ non-zero elements in each vector. This results in a sparsity factor of $\frac{K}{Nn_tM} = \frac{6}{1024}$. This sparsity can be exploited for efficient signal detection using sparse recovery algorithms.

### *A. Sparsity-exploiting signal detection*

Several sparse recovery algorithms are known in the literature [35]-[37]. A sparse recovery algorithm seeks solution to the following problem:

$$\min_{\mathbf{x}} \|\mathbf{x}\|_0 \text{ subject to } \mathbf{b} = \mathbf{A}\mathbf{x} + \mathbf{n}, \tag{15}$$

where $\mathbf{A} \in \mathbb{C}^{m \times n}$ is the called the sensing matrix, $\mathbf{b} \in \mathbb{C}^{m \times 1}$ is the noisy observation corresponding to the input vector $\mathbf{x} \in \mathbb{C}^{n \times 1}$, and $\mathbf{n} \in \mathbb{C}^{m \times 1}$ is the complex noise vector. The sparse nature of the index modulation transmit vectors allows us to model the signal detection problem at the receiver as a sparse recovery problem of the form (15). In our detection problem, the sensing matrix $\mathbf{A}$ in (15) is the channel matrix $\mathbf{H}$, the noisy observation $\mathbf{b}$ is the received signal vector $\mathbf{y}$, and the goal is to detect the sparse transmit vector $\mathbf{x}$. We adapt greedy sparse recovery algorithms such as orthogonal matching pursuit (OMP) [35], compressed sampling matching

**Algorithm 1** Sparsity-exploiting detection algorithm

1: Inputs: $\mathbf{y}, \mathbf{H}, K, \mathbb{T}$
2: Initialize: $j = 0$
3: **repeat**
4: $\quad \hat{\mathbf{x}}_r = \text{SR}(\mathbf{y}, \mathbf{H}, K + j)$ ▷ Sparse recovery algorithm
5: $\quad \mathbf{t}^{\hat{\mathbf{x}}_r,(j)} = \text{TAP}(\hat{\mathbf{x}}_r)$ ▷ Extract TAP
6: $\quad$ **if** $\|\mathbf{t}^{\hat{\mathbf{x}}_r,(j)}\|_0 = K$ and $\mathbf{t}^{\hat{\mathbf{x}}_r,(j)} \in \mathbb{T}$
7: $\quad\quad$ **for** $k = 1$ to $N$
8: $\quad\quad\quad \hat{\mathbf{x}}^k = \underset{\mathbf{s}\in\mathbb{S}_{\text{sm-mbm}}}{\text{argmin}} \ \|\hat{\mathbf{x}}_r^k - \mathbf{s}\|^2, \quad \text{if } t_k^{\hat{\mathbf{x}}_r,(j)} = 1$
$\quad\quad\quad\quad\quad = \mathbf{0}, \qquad\qquad\quad \text{if } t_k^{\hat{\mathbf{x}}_r,(j)} = 0$
9: $\quad\quad$ **end for**
10: $\quad\quad$ **break**; ▷ break repeat loop
11: $\quad$ **else** $j = j + 1$
12: $\quad$ **end if**
13: **until** $j < (Nn_tM - K)$
14: Output: Estimated TI-SM-MBM signal vector

$$\hat{\mathbf{x}} = [\hat{\mathbf{x}}^{1^T}\ \hat{\mathbf{x}}^{2^T} \cdots\ \hat{\mathbf{x}}^{N^T}]^T$$

pursuit (CoSaMP) [36], and subspace pursuit (SP) [37] for our purpose. For an $m \times n$ sensing matrix and a $k$-sparse vector, the reconstruction complexity of these algorithms is $\mathcal{O}(kmn)$. **Algorithm 1** lists the sparsity-exploiting detection algorithm for TI-SM-MBM.

In **Algorithm 1**, SR denotes sparse recovery algorithm, which can be any one of OMP, CoSaMP, SP. The signal vector reconstructed by SR is denoted by $\hat{\mathbf{x}}_r$. Detecting a TI-SM-MBM signal vector involves $i$) obtaining a valid TAP and $ii$) detecting the SM-MBM signal vector in each active time slot. In a given iteration $j$, the estimated TAP, $\mathbf{t}^{\hat{\mathbf{x}}_r,(j)}$, is obtained from the received vector as follows. A TI-SM-MBM signal vector consists of SM-MBM signal vectors in $K$ active time slots and zero vectors in $N - K$ inactive time slots. The SM-MBM signal vector in an active time slot consists of only one non-zero element. Hence, SR is expected to reconstruct $\hat{\mathbf{x}}_r$ with exactly one non-zero element in the subvector of each active time slot. This constraint on the expected support set is not incorporated in the standard sparse recovery algorithms. A standard sparse recovery algorithm can output a vector with $K$ non-zero entries in any of the $Nn_tM$ positions of $\hat{\mathbf{x}}_r$. In order to extract TAP from $\hat{\mathbf{x}}_r$, the algorithm treats a time slot with at least one non-zero entry in the subvector of that time slot to be an active time slot. In order to identify the $K$ active time slots in the TI-SM-MBM signal vector, SR is used multiple times over a range of sparsity values starting from $K$. The TAP vector corresponding to $\hat{\mathbf{x}}_r$ in the $j$th iteration is obtained such that $t_k^{\hat{\mathbf{x}}_r,(j)} = 1$ if $k$th slot is active and zero otherwise. The input sparsity value is incremented by one till a valid TAP is obtained. On recovering an $\hat{\mathbf{x}}_r$ with valid TAP, the subvector in each active time slot is mapped to the SM-MBM signal vector which is nearest in the Euclidean sense (i.e., to the nearest vector in $\mathbb{S}_{\text{sm-mbm}}$ ). This is shown in Step 8 of the algorithm, where $\hat{\mathbf{x}}_r^k$ denotes the $n_tM \times 1$-length recovered subvector in the $k$th time slot and $\hat{\mathbf{x}}^k$ is the signal vector to which $\hat{\mathbf{x}}_r^k$ gets mapped. The detected TI-SM-MBM signal vector output from the algorithm is $\hat{\mathbf{x}} = [\hat{\mathbf{x}}^{1^T}\ \hat{\mathbf{x}}^{2^T} \cdots \hat{\mathbf{x}}^{N^T}]^T$. The decoding of information bits from $\hat{\mathbf{x}}$ involves obtaining time-slot index bits, mirror index bits, antenna index bits, and QAM symbol bits. The time-slot index bits are decoded from the indices of active time slots in $\hat{\mathbf{x}}$ using combinadics based decoding [7]. The mirror index bits and antenna index bits are decoded from the detected SM-MBM signal vectors in active time slots. The detected SM-MBM signal vector also gives the QAM symbol being transmitted, from which QAM bits can be decoded.

We note that **Algorithm 1** can be used for the detection of TI-SM, TI-MBM, and SM-MBM, as they are special cases of TI-SM-MBM. The only change is in the nearest symbol mapping in Step 8, where $\hat{x}_r^k$ has to be mapped to the nearest SM signal vector from $\mathbb{S}_{\text{sm}}$ for TI-SM and to the nearest MBM signal vector from $\mathbb{S}_{\text{mbm}}$ for TI-MBM.

### *B. Performance results*

This subsection presents the BER performance of the various index modulation schemes with OMP, CoSaMP, and SP based detection.

*1) TI-SM-MBM performance with OMP, CoSaMP, SP:* In Fig. 3, we present the BER performance of TI-SM-MBM with OMP, CoSaMP, and SP based signal detection. The considered TI-SM-MBM scheme uses $N = 16, K = 6, n_t = 8, n_r = 8, m_{rf} = 4$, and 4-QAM. The number of multipaths considered is $L = 4$, and the achieved rate is 3.47 bpcu. From Fig. 3, it can be seen that SP and CoSaMP based detection achieve superior performance compared to OMP based detection. While the BER floors at around $10^{-4}$ with OMP, it falls much below $10^{-4}$ with CoSaMP and SP. Between SP and CoSaMP, SP has superior reconstruction performance. This can be seen from the SNR advantage of about 1.5 dB at $10^{-5}$ BER in favor of SP based detection compared to CoSaMP based detection.

*2) TI-SM, TI-MBM, SM-MBM, TI-SM-MBM performance with SP based detection:* In Fig. 4, we present the BER performance of TI-SM, TI-MBM, SM-MBM and TI-SM-MBM with SP based detection. All the four schemes use $N = 16$ and $n_r = 8$. The number of multipaths is $L = 4$. The SM-MBM scheme achieves 3.36 bpcu using $n_t = 4, m_{rf} = 1$, and BPSK. The TI-SM, TI-MBM, and SM-MBM schemes achieve 3.47 bpcu using the following configurations: $i$) TI-SM: $K = 6, n_t = 16$, and 32-QAM, $ii$) TI-MBM: $K = 6, n_t = 1, m_{rf} = 5$, and 16-QAM, and $iii$) TI-SM-MBM: $K = 6, n_t = 4, m_{rf} = 5$, and 4-QAM. It can be seen from Fig. 4 that SM-MBM and TI-SM-MBM schemes have superior performance compared to TI-SM and TI-MBM schemes. Also, TI-SM-MBM performs the best among all the considered schemes. We can see that this comparative performance behavior of the considered schemes for large-dimension systems ($N = 16, K = 6$, length of the signal vectors: $2^8$ to $2^{11}$) with SP based detection is similar in trend

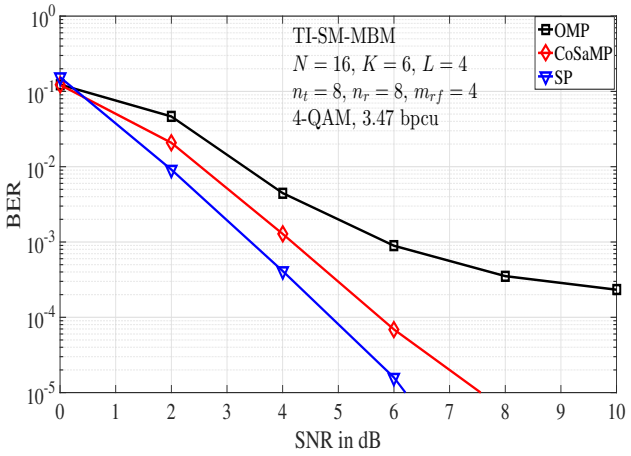


Fig. 3. BER performance of TI-SM-MBM with OMP, CoSaMP, and SP based detection. $N = 16$, $K = 6$, $n_t = 8$, $n_r = 8$, $m_{rf} = 4$, 4-QAM, $L = 4$, 3.47 bpcu.

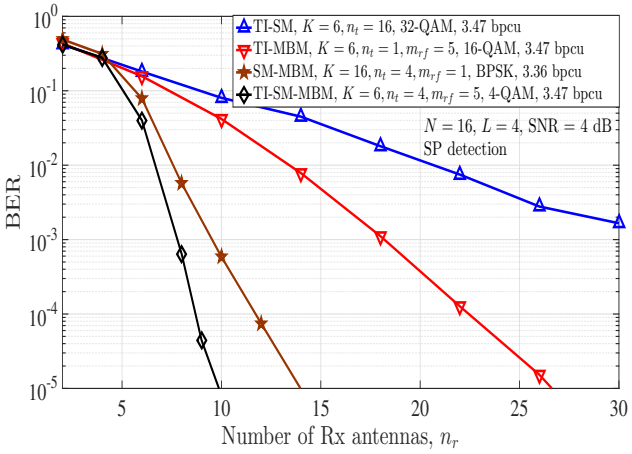


Fig. 5. BER performance of TI-SM, TI-MBM, SM-MBM, and TI-SM-MBM schemes as a function of $n_r$ with SP based detection at SNR = 4 dB.

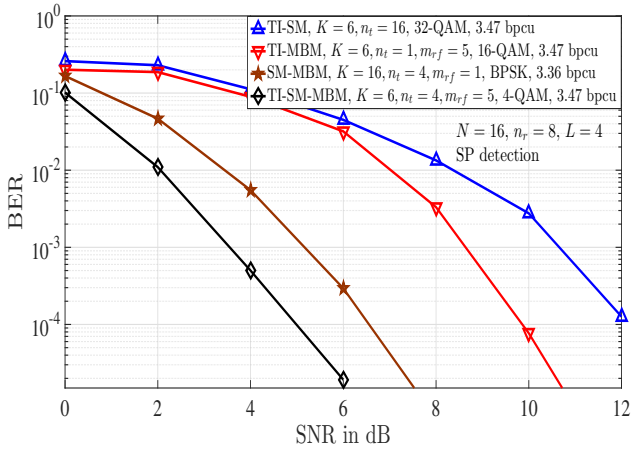


Fig. 4. BER performance comparison of TI-SM, TI-MBM, SM-MBM, and TI-SM-MBM schemes with SP based detection.

compared to what was observed for small-dimension systems ($N = 4, K = 2$, length of the signal vectors: $2^4$ to $2^7$) with ML detection in Fig. 2. The reasoning we presented in Sec. II-E for the relative performance in Fig. 2 applies here as well.

*3) Effect of the number of receive antennas, $n_r$:* In Fig. 5, we present the BER performance of TI-SM, TI-MBM, SM-MBM and TI-SM-MBM schemes as a function of number of receive antennas at an SNR of 4 dB. It can be seen that the BER performance of TI-SM-MBM improves drastically with the increase in number of receive antennas compared to other schemes. TI-SM-MBM requires $n_r = 9$ receive antennas to achieve a BER of $10^{-4}$, whereas SM-MBM requires $n_r = 12$ and TI-MBM requires $n_r = 22$ receive antennas to achieve the same BER. TI-SM exhibits poor performance with an error floor above $10^{-4}$ BER. These results illustrate that indexing increased number of transmit entities (e.g., as in TI-SM-MBM) can render the possibility of achieving a reduction in the required number of receive antennas at the receiver.

## IV. Indexed Load Modulation

In this section, we first introduce the concept of load modulation for multiantenna systems [30],[31], and then present two indexing schemes for load modulated systems, namely, spatially-indexed load modulation (SI-LM) and time-indexed load modulation (TI-LM).

### A. Load modulation for multiantenna systems

In conventional RF transmitter hardware, circuit impedance is kept constant and a voltage is formed proportional to the information bearing signal. This is called the traditional 'voltage modulation'. It has the advantage that the circuit impedance can be matched to the antenna load impedance for optimum power transfer. A disadvantage, however, is that the PA needs to be backed-off considerably to ensure a linear response over the entire input voltage range. In spatially multiplexed multiantenna systems, separate PAs in each RF chain must be driven at high back-offs. RF hardware cost and power efficiency concerns thus become impediments to the deployment of massive antenna arrays.

Load modulation array refers to an array architecture wherein the antenna load impedances are chosen to be proportional to the information bearing signals while being driven by a sinusoid of fixed amplitude and phase and a single central power amplifier (CPA) [30]. Referring to a multiantenna transmitter, the load impedance in the $l$th antenna, $Z_l(t)$, is chosen to be proportional to the $l$th transmit signal $s_l(t)$, $l = 1, 2, \cdots, n_t$. The circuit that achieves this is called a load modulator. A load modulator can be implemented by means of varactor diodes or pin-diodes. Load modulation thus generates input currents to the antennas based on information bearing signals, in effect implementing the desired constellation in the analog domain [30]. Figure 6 shows a load modulation array.

The effective admittance seen by the power source is the sum of the admittances of all antenna loads, i.e., $Y(t) = \sum_{l=1}^{n_t} \frac{1}{Z_l(t)}$. The single power source becomes equivalent to $n_t$ parallel power sources, each with an average admittance

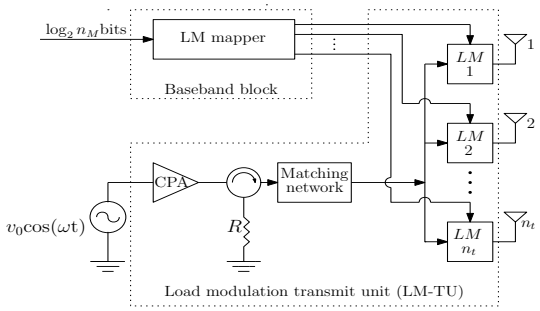


Fig. 6. Load modulation array.

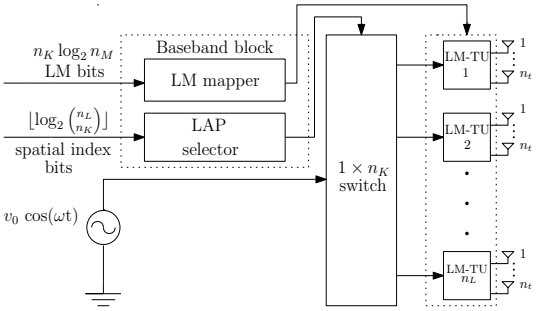


Fig. 7. Spatially-indexed load modulation scheme.

$Y(t)/n_t$. Since $Y(t)$ varies with the information bearing signals, there may be a mismatch between circuit impedance and effective antenna impedance, and so power may be reflected back to the CPA. A circulator is therefore used to redirect any reflected power to a resistor $R$. For massive antenna arrays (large $n_t$), the law of large numbers ensures that the average admittance $Y(t)/n_t$ does not vary much even while the individual admittances may vary significantly. So the circuit impedance can be matched to the average impedance, which results in only a small power being reflected back to the CPA. We term the assembly of the CPA, circulator, and $n_t$ antennas and their associated load modulators as a *load modulation transmit unit* (LM-TU) – see Fig. 6.

The efficiency of the CPA in an LM-TU is determined by the peak to average sum power ratio (PASPR), which is the peak to average power ratio (PAPR) aggregated over all the antenna elements [32]. For massive antenna arrays, the PASPR tends asymptotically to one due to law of large numbers, and therefore the CPA can be operated at its highest efficiency. For small number of antennas, however, the PASPR can be more than one. To obtain a PASPR close to one with small number of antennas, it is desired that the sum power radiated by the antennas be made constant. A way to achieve this is to use phase modulation on the hypersphere (PMH) [32].

PMH uses points on the $n_t$-dimensional hypersphere to form the LM alphabet. Let $\mathbb{S}_{\text{lm}}$ denote the $n_M$-ary LM alphabet, where $n_M \triangleq |\mathbb{S}_{\text{lm}}|$. Let $\mathbb{S}_{\text{H}}(n_t, P) = \{\mathbf{s} \in \mathbb{C}^{n_t} \mid \|\mathbf{s}\|^2 = P\}$ denote the $n_t$-dimensional complex-valued hypersphere of radius $\sqrt{P}$. Then, $\mathbb{S}_{\text{lm}} = \{\mathbf{s}_1, \mathbf{s}_2, \cdots, \mathbf{s}_{n_M}\} \subset \mathbb{S}_{\text{H}}(n_t, P)$. One way to obtain the signal vectors that constitute $\mathbb{S}_{\text{lm}}$ is by generating uniformly distributed vectors on the hypersphere and clustering them [32]. An $n_t \times 1$ signal vector $\mathbf{s}$ from $\mathbb{S}_{\text{lm}}$ chosen based on $\log_2 n_M$ information bits gets transmitted in a channel use by the $n_t$ load modulators as shown in Fig. 6.

### *B. Spatially-indexed load modulation (SI-LM)*

It is noted that an LM-TU would require a higher peak-power rated CPA as the number of loads driven by it (i.e., $n_t$) is increased. For example, it has been shown in [31] that an LM-TU with $n_t = 100$ requires its CPA to have a peak-power rating which is about 21 times more than that of a per-stream PA in a conventional multiantenna system using spatial multiplexing with $n_t = 100$. A higher peak-power rated CPA poses challenges in terms of its thermal design and number of gain stages [38]. A tradeoff thereby arises between PASPR (which requires a large antenna array) and peak-power rating of the CPA (whose design prefers small number of antennas/loads). A desirable configuration would then be to have multiple LM-TUs, say $n_L$ LM-TUs, each with a CPA that has a lower peak-power rating requirement. Transmit signals from all the LM-TUs could consequently be spatially multiplexed to obtain the same transmit sum power. While this spatial multiplexing of signals from multiple LM-TUs is one possibility, another interesting possibility is to spatially index the multiple LM-TUs. Such a scheme, which we call spatially-indexed LM (SI-LM) scheme, is presented in the following.

Consider a transmitter equipped with $n_L$ LM-TUs, each employing $n_t$ antennas (Fig. 7). Every LM-TU is configured to generate an $n_M$-ary alphabet on the $n_t$-dimensional hypersphere via load modulation. Of the $n_L$ LM-TUs, $n_K$ LM-TUs are activated in each channel use. The remaining $n_L - n_K$ LM-TUs remain inactive (i.e., OFF). A $1 \times n_K$ switch connects the oscillator output to the $n_K$ active LM-TUs. An $n_L$-length pattern of active/inactive status of the LM-TUs is called a LM-TU activation pattern (LAP). The LAP for a given channel use is chosen based on by $\lfloor \log_2 \binom{n_L}{n_K} \rfloor$ bits. These bits are called the spatial-index bits. On each active LM-TU, an LM signal vector from $\mathbb{S}_{\text{lm}}$ is transmitted so that $n_K \log_2 n_M$ bits (called the LM bits) are conveyed by the $n_K$ active LM-TUs. The achieved rate in the SI-LM scheme therefore is given by

$$\eta_{\text{si-lm}} = \left\lfloor \log_2 \binom{n_L}{n_K} \right\rfloor + n_K \log_2 n_M \quad \text{bpcu.} \tag{16}$$

The SI-LM alphabet, denoted by $\mathbb{S}_{\text{si-lm}}$, which is the set of all $n_L n_t \times 1$-sized vectors that can be transmitted is given by

$$\begin{aligned} \mathbb{S}_{\text{si-lm}} = \big\{ \mathbf{s} = [\mathbf{s}_1^T \mathbf{s}_2^T \cdots \mathbf{s}_{n_L}^T]^T : \mathbf{s}_j \in \mathbb{S}_{\text{lm}} \cup \mathbf{0}_{n_t}, \\ \|\mathbf{s}\|_0 = n_K n_t, \ \mathbf{q}^{\mathbf{s}} \in \mathbb{L} \big\}, \end{aligned} \tag{17}$$

where $\mathbf{s}_j$ is the $n_t \times 1$ transmitted vector from the $j$th LM-TU, $\mathbb{S}_{\text{lm}}$ is the $n_M$-ary LM alphabet, $\mathbf{0}_{n_t}$ is an $n_t \times 1$ vector of zeros, $\|\mathbf{s}\|_0$ is the $l_0$-norm of $\mathbf{s}$, $\mathbf{q}^{\mathbf{s}}$ is the LAP corresponding to $\mathbf{s}$, and $\mathbb{L}$ is the set of all valid LAPs.

Assuming $n_r$ antennas at the receiver, the received signal vector $\mathbf{y}$ can be written as $\mathbf{y} = \mathbf{H}\mathbf{s} + \mathbf{n}$, where $\mathbf{H}$ denotes the $n_r \times n_L n_t$ matrix of channel gains such that the gain from the $j$th transmit antenna to the $i$th receiver antenna

$h_{ij} \sim \mathcal{CN}(0,1)$ and $\mathbf{n}$ is the $n_r \times 1$ noise vector with $\mathbf{n} \sim \mathcal{CN}(0, \sigma^2\mathbf{I})$.

*ML detection performance:* In Fig. 8, we present the BER performance of various SI-LM and spatially-multiplexed LM (SMP-LM) schemes under ML detection. All schemes are configured to achieve 8 bpcu and have $n_r = 16$. We also present the BER performance of conventional LM without indexing ($n_L = 1$) and conventional SMP (i.e., SMP without LM) that achieve 8 bpcu. Every LM-TU is assumed to have $n_t = 8$ antennas (loads). The required LM alphabets are obtained on the $n_t$-dimensional hypersphere using the spherical k-means clustering (kMC) algorithm [32],[39]. The following observations can be made from Fig. 8.

- At $10^{-4}$ BER, we observe that conventional LM (without indexing) performs better by about 2 dB compared to conventional SMP with BPSK. By using a signaling alphabet that is simultaneously optimized over $n_t = 8$ dimensions, LM is able to achieve this better performance compared to conventional SMP that operates with a per dimension signaling alphabet.
- When the transmitter is equipped with multiple LM-TUs ($n_L > 1$), SI-LM performs better than SMP-LM. For example, SI-LM with $n_L = 4, n_K = 1$, and $n_M = 64$ performs better by about 2.5 dB compared to SMP-LM with $n_L = 4, n_K = 4$, and $n_M = 4$. Note that SI-LM achieves this improved performance despite using a larger alphabet size (i.e., $n_M = 64$ and 4 for SI-LM and SMP-LM, respectively). This is because the effect of spatial interference in SMP-LM outweighs the effect of adding more signal points on the hypersphere in SI-LM. Also, the SNR advantage of SI-LM over SMP-LM increases with $n_L$ since number of index bits increases with increased number of LM-TUs.

### C. Time-indexed load modulation (TI-LM)

Motivated by the performance gains offered by time indexing in SM and MBM (in Sec. II), here, we investigate the potential performance benefits of time indexing in LM. Towards this, we consider a system model which similar to the model considered for TI-SM and TI-MBM in Sec. II. The channel is assumed to be frequency selective with $L$ multipaths. Each transmission frame consists of $N + L - 1$ time slots, with $N$ slots for data transmission and $L - 1$ slots for CP. Of the $N$ time slots, only $K$ slots are used for data transmission. The remaining $N - K$ slots stay silent. The choice of which $K$ slots among the $N$ slots are selected for transmission conveys $\lfloor \log_2 \binom{N}{K} \rfloor$ information bits. These bits are called 'time index bits' and the selected time slots are called 'active slots' in the frame. An $N$-length pattern of active/inactive status of the slots in a frame is called a 'time-slot activation pattern' (TAP). There are $\binom{N}{K}$ possible TAPs, of which $2^{\lfloor \log_2 \binom{N}{K} \rfloor}$ are used and they form the set of valid TAPs. On each active slot, an LM signal vector from $\mathbb{S}_{\text{lm}}$ is transmitted so that $K \log_2 n_M$ bits are conveyed in $K$ active slots. The achieved rate in the TI-LM scheme is given by

$$\eta_{\text{ti-lm}} = \frac{1}{N + L - 1} \left[ \left\lfloor \log_2 \binom{N}{K} \right\rfloor + K \log_2 n_M \right] \quad \text{bpcu.}$$

The TI-LM alphabet, denoted by $\mathbb{S}_{\text{ti-lm}}$, is the set of $Nn_t \times 1$-sized vectors obtained by concatenating $N$ vectors each of size $n_t \times 1$, as follows:

$$\mathbb{S}_{\text{ti-lm}} = \{ \mathbf{s} = [\mathbf{s}_1^T \mathbf{s}_2^T \cdots \mathbf{s}_N^T]^T : \mathbf{s}_j \in \mathbb{S}_{\text{lm}} \cup \mathbf{0}_{n_t}, \; \|\mathbf{s}\|_0 = Kn_t, \; \mathbf{t}^{\mathbf{s}} \in \mathbb{T} \}, \tag{18}$$

where $\mathbb{T}$ denotes the set of valid TAPs and $\mathbf{t}^{\mathbf{s}}$ denotes the TAP corresponding to $\mathbf{s}$. An $Nn_t \times 1$ TI-LM signal vector from $\mathbb{S}_{\text{ti-lm}}$ is transmitted over $N$ slots in a frame.

The channel is assumed to remain constant over one frame duration and to be perfectly known at the receiver. After the removing the CP, the $Nn_r \times 1$ received signal vector can be written as $\mathbf{y} = \mathbf{H}\mathbf{s} + \mathbf{n}$, where $\mathbf{n}$ is $Nn_r \times 1$ noise vector with $\mathbf{n} \sim \mathcal{CN}(\mathbf{0}, \sigma^2\mathbf{I})$ and $\mathbf{H}$ is $Nn_r \times Nn_t$ equivalent block circulant matrix having the same form and statistics as in (6).

*ML detection performance:* In Fig. 9, we present the BER performance of TI-LM scheme with $N = 4$, $K = 2$, $n_t = 8$, $n_M = 32$, $L = 2$, and 2.4 bpcu. The performance of conventional LM (without time indexing) with the same 2.4 bpcu is also presented for comparison. The conventional LM achieves 2.4 bpcu using $N = 4$, $n_t = 8$, $n_M = 8$, $L = 2$. Both systems use $n_r = 8$ and ML detection. The LM alphabets are obtained from the spherical kMC algorithm as before. At $10^{-4}$ BER, it is seen that TI-LM performs better by about 1.5 dB compared to conventional LM without time indexing, which is due to reduced ISI in TI-LM.

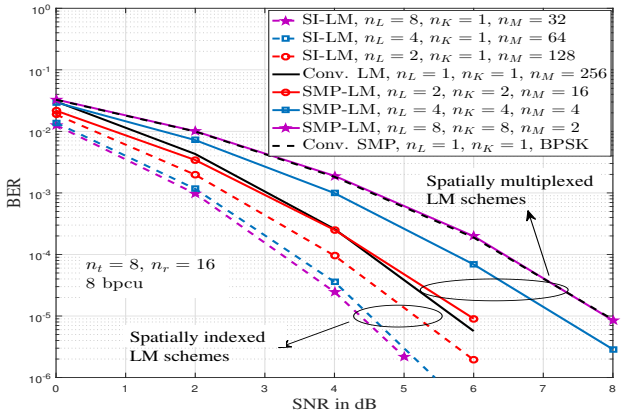


Fig. 8. BER performance of spatially-indexed LM and spatially-multiplexed LM with $n_t = 8$, $n_r = 16$, and 8 bpcu in flat fading with ML detection. Conventional LM and SMP performance are also shown.

## V. Conclusions

Conveying information bits through indexing transmission entities is an efficient signaling approach. In this paper, we presented index modulation schemes in which transmit antennas, time slots, and RF mirrors are indexed simultaneously. ML detection performance of these schemes pointed to very good performance possible through indexing of multiple entities.

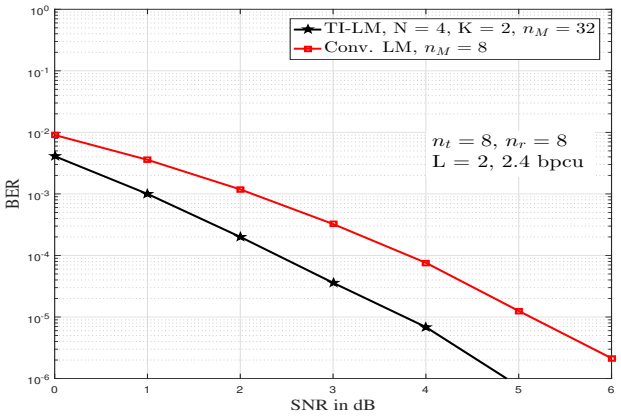


Fig. 9. BER performance of time-indexed LM in frequency selective fading with $N = 4$, $K = 2$, $n_t = 8$, $n_M = 32$, $L = 2$, 2.4 bpcu, $n_r = 8$, and ML detection. Conventional LM performance is also shown.

To enable the detection of large-dimension signals of these schemes, we exploited the inherent sparsity present in their signal vectors. Detection using sparsity-exploiting compressive sensing algorithms also showed attractive performance. The results indicate that indexing multiple transmission entities with a careful choice of system configuration/parameters exploiting the underlying tradeoffs involved can be beneficial. We also explored the potential benefits of indexing in load modulation. Indexing space and time showed promising performance gains in load modulated multiantenna systems.

## REFERENCES


[1] E. Basar, "Index modulation techniques for 5G wireless networks," *IEEE Commun. Mag.*, vol. 54, no. 7, pp. 168-175, Jul. 2016.

[2] Y. A. Chau and S.-H. Yu, "Space modulation on wireless fading channels," in *Proc. IEEE VTC-Fall*, vol. 3, Oct. 2001, pp. 1668-1671.

[3] R. Mesleh, H. Haas, S. Sinanovic, C. W. Ahn, and S. Yun, "Spatial modulation," *IEEE Trans. Veh. Tech.*, vol. 57, no. 4, pp. 2228-2241, Jul. 2008.

[4] M. Di Renzo, H. Haas, A. Ghrayeb, S. Sugiura, and L. Hanzo, "Spatial modulation for generalized MIMO: Challenges, opportunities and implementation," *Proceedings of the IEEE*, vol. 102, no. 1, pp. 56-103, Jan. 2014.

[5] J. Wang, S. Jia, and J. Song, "Generalised spatial modulation system with multiple active transmit antennas and low complexity detection scheme," *IEEE Trans. Wireless Commun.*, vol. 11, no. 4, pp. 1605-1615, Apr. 2012.

[6] T. Datta and A. Chockalingam, "On generalized spatial modulation," in *Proc. IEEE WCNC*, Apr. 2013, pp. 2716-2721.

[7] T. Lakshmi Narasimhan and A. Chockalingam, "On the capacity and performance of generalized spatial modulation," *IEEE Commun. Lett.*, vol. 20, no. 2, pp. 252-255, Feb. 2015.

[8] N. Serafimovski1, S. Sinanovic, M. Di Renzo, and H. Haas, "Multiple access spatial modulation," *EURASIP J. Wireless Commun. Netw.*, vol. 299, Sep. 2012.

[9] T. Lakshmi Narasimhan, P. Raviteja, and A. Chockalingam, "Large-scale multiuser SM-MIMO versus massive MIMO," in *Proc. ITA*, Feb. 2014, pp. 1-9.

[10] P. Yang, Y. Xiao, K. V. S. Hari, A. Chockalingam, S. Sugiura, H. Haas, M. Di Renzo, Z. Liu, L. Xiao, S. Li, and L. Hanzo, "Single-carrier spatial modulation: a promising design for large-scale broadband antenna systems," *IEEE Commun. Surveys & Tutorials*, vol. 18, no. 3, pp. 1687-1716, 3rd quarter, 2016.

[11] T. Lakshmi Narasimhan, P. Raviteja, and A. Chockalingam, "Generalized spatial modulation in large-scale multiuser MIMO systems," *IEEE Trans. Wireless Commun.*, vol. 14, no. 7, pp. 3764-3779, Jul. 2015.

[12] N. Ishikawa, R. Rajashekar, S. Sugiura, and L. Hanzo, "Generalized spatial modulation based reduced-RF-Chain millimeter wave communications," *IEEE Trans. Veh. Tech.*, vol. 66, no. 1, pp. 879-883, Jan. 2017.

[13] G. D. Surabhi and A. Chockalingam, "Efficient signaling schemes for mmWave LOS MIMO communication using uniform linear and circular arrays," to appear in *Proc. IEEE VTC-Spring*, Jun. 2017.

[14] R. Abu-alhiga and H. Haas, "Subcarrier index modulation OFDM," in *Proc. IEEE PIMRC*, Sep. 2009, pp. 177-181.

[15] E. Basar, U. Aygolu, E. Panayirci, and H. V. Poor, "Orthogonal frequency division multiplexing with index modulation," *IEEE Trans. Signal Process.*, vol. 61, no. 22, pp. 5536-5549, Nov. 2013.

[16] Y. Xiao, S. Wang, L. Dan, X. Lei, P. Yang, and W. Xiang, "OFDM with interleaved subcarrier-index modulation," *IEEE Commun. Lett.*, vol. 8, no. 8, pp. 1447-1450, Aug. 2014.

[17] E. Basar, "On multiple-input multiple-output OFDM with index modulation for next generation wireless networks," *IEEE Trans. Signal Process.*, vol. 64, no. 15, pp. 3868-3878, Aug. 2016.

[18] N. Ishikawa, S. Sugiura, and L. Hanzo, "Subcarrier-index modulation aided OFDM - will it work?," *IEEE Access*, vol. 4, pp. 2580-2593, 2016.

[19] H. Zhang, L-L. Yang, and L. Hanzo, "Compressed sensing improves the performance of subcarrier index-modulation-assisted OFDM," *IEEE Access*, vol. 4, pp. 7859-7873, 2016.

[20] T. Datta, H. Eshwaraiah, and A. Chockalingam, "Generalized space-and-frequency index modulation," *IEEE Trans. Veh. Tech.*, vol. 65, no. 7, pp. 4911-4924, Jul. 2016.

[21] S. Sugiura, S. Chen, and L. Hanzo, "Generalized space-time shift keying designed for flexible diversity-, multiplexing- and complexity-tradeoffs," *IEEE Trans. Wireless Commun.*, vol. 10, no. 4, pp. 1144-1153, Apr. 2011.

[22] T. Lakshmi Narasimhan, Y. Naresh, T. Datta, and A. Chockalingam, "Pseudo-random phase precoded spatial modulation and precoder index modulation," in *Proc. IEEE GLOBECOM*, Nov. 2014, pp. 3868-3873.

[23] Y. Naresh, T. Lakshmi Narasimhan, and A. Chockalingam, "Capacity bounds and performance of precoder index modulation," in *Proc. IEEE WCNC*, Apr. 2016, pp. 1-6.

[24] O. N. Alrabadi, A. Kalis, C. B. Papadias, R. Prasad, "Aerial modulation for high order PSK transmission schemes," in *Proc. Wireless VITAE*, May 2009, pp. 823-826.

[25] O. N. Alrabadi, A. Kalis, C. B. Papadias, and R. Prasad, "A universal encoding scheme for MIMO transmission using a single active element for PSK modulation schemes," *IEEE Trans. Wireless Commun.*, vol. 8 , no. 10, pp. 5133-5142, Oct. 2009.

[26] A. K. Khandani, "Media-based modulation: a new approach to wireless transmission," in *Proc. IEEE ISIT*, Jul. 2013, pp. 3050-3054.

[27] A. K. Khandani, "Media-based modulation: converting static Rayleigh fading to AWGN," in *Proc. IEEE ISIT*, Jun-Jul. 2014, pp. 1549-1553.

[28] E. Seifi, M. Atamanesh, and A. K. Khandani, "Media-based MIMO: outperforming known limits in wireless," in *Proc. IEEE ICC*, May 2016, pp. 1-7.

[29] Y. Naresh and A. Chockalingam, "On media-based modulation using RF mirrors," *IEEE Trans. Veh. Tech.*, 2016. Available IEEE Xplore: DOI: 10.1109/TVT.2016.2620989.

[30] M. A. Sedaghat, V. I. Barousis, R. R. Muller, and C. B. Papadias, "Load modulated arrays: a low-complexity antenna," *IEEE Commun. Mag.*, pp. 46-52, Mar. 2016.

[31] R. R. Muller, M. A. Sedaghat, and G. Fischer, "Load modulated massive MIMO," in *Proc. IEEE GlobalSIP*, pp. 622-626, Dec. 2014.

[32] M. A. Sedaghat, R. R. Muller, and C. Rachinger, "(Continuous) phase modulation on the hypersphere," *IEEE Trans. Wireless Commun.*, vol. 15, no. 8, pp. 5763-5774, Aug. 2016.

[33] S. Jacob, T. Lakshmi Narasimhan, and A. Chockalingam, "Space-time index modulation," to appear in *Proc. IEEE WCNC*, Mar. 2017.

[34] B. Shamasundar, S. Jacob, and A. Chockalingam, "Time-indexed media-based modulation," to appear in *Proc. IEEE VTC-Spring*, Jun. 2017.

[35] J. A. Tropp and A. C. Gilbert, "Signal recovery from random measurements via orthogonal matching pursuit," *IEEE Trans. Inform. Theory*, vol. 53, vol. 12, pp. 4655-4666, Dec. 2007.

[36] D. Needell and J. A. Tropp, "CoSaMP: iterative signal recovery from incomplete and inaccurate samples," *Applied and Computational Harmonic Analysis*, 26.3 (2009): 301-321.

[37] W. Dai and O. Milenkovic, "Subspace pursuit for compressive sensing signal reconstruction," *IEEE Trans. Inform. Theory*, vol. 55, no. 5, pp. 2230-2249, May 2009.

[38] S. C. Cripps, *RF Power Amplifiers for Wireless Communications*, 2nd Ed., Artech House, 2006.

[39] I.S. Dhillon and D. S. Modha, "Concept decompositions for large sparse text data using clustering," *Machine Learning*, vol. 42, no. 1, pp. 143-175, Jan. 2001.